Supporting Information for *"A Collapsible Soft Actuator Facilitates Performance in Constrained Environments"*

*Jacob Rogatinsky Kiran Gomatam Zi Heng Lim Megan Lee Lorenzo Kinnicutt Christian Duriez Perry Thomson Kevin McDonald Tommaso Ranzani**

Supporting Information

This file includes:

Derivation of the geometric model
Mathematica code for the derivation of the geometric model
Details on the real-time FEM model in SOFA
Details on the gravitational contribution to force testing
Details on the ABAQUS simulation to estimate the SBA's stiffness
Details on the experimental setup
Figure S1
Figure S2
Figure S3

S1 Geometric Model

To derive the geometric model for SBA inflation, we fit a variety of curves to a cross section of an individual SBA balloon using MATLAB image processing (Figure S1). We analyzed circles, ellipses, and parabolas, and we found that parabolas generated the closest fit to the shape of the balloon's cross section.
We therefore attempted to approximate a relationship between the volume of fluid inside a balloon, and the resulting height of the balloon.
To do this, we developed a system of three equations reported below a well as in Figure S1.

$$v = 2\pi \int_0^{\rho} x(h - \alpha x^2)dx \tag{1}$$

$$y(x = \rho) = 0 = h - \alpha\rho^2 \tag{2}$$

$$l = \int_0^{\rho} \sqrt{1 + (-2\alpha\rho)^2}dx \tag{3}$$

The first equation (Eq.1) describes the volume inside the balloon, approximated as the volume of revolution created by rotating a parabola about the y-axis and multiplying by 2 to account for both halves of the balloon.
The second equation (Eq.2) is a boundary condition, stating that $y = 0$ when $x = \rho$.
The third equation (Eq.3) puts a constraint on the arc length of the cross sectional boundary, by setting the arc length of the parabola in the first quadrant equal to the deflated radius of the balloon.

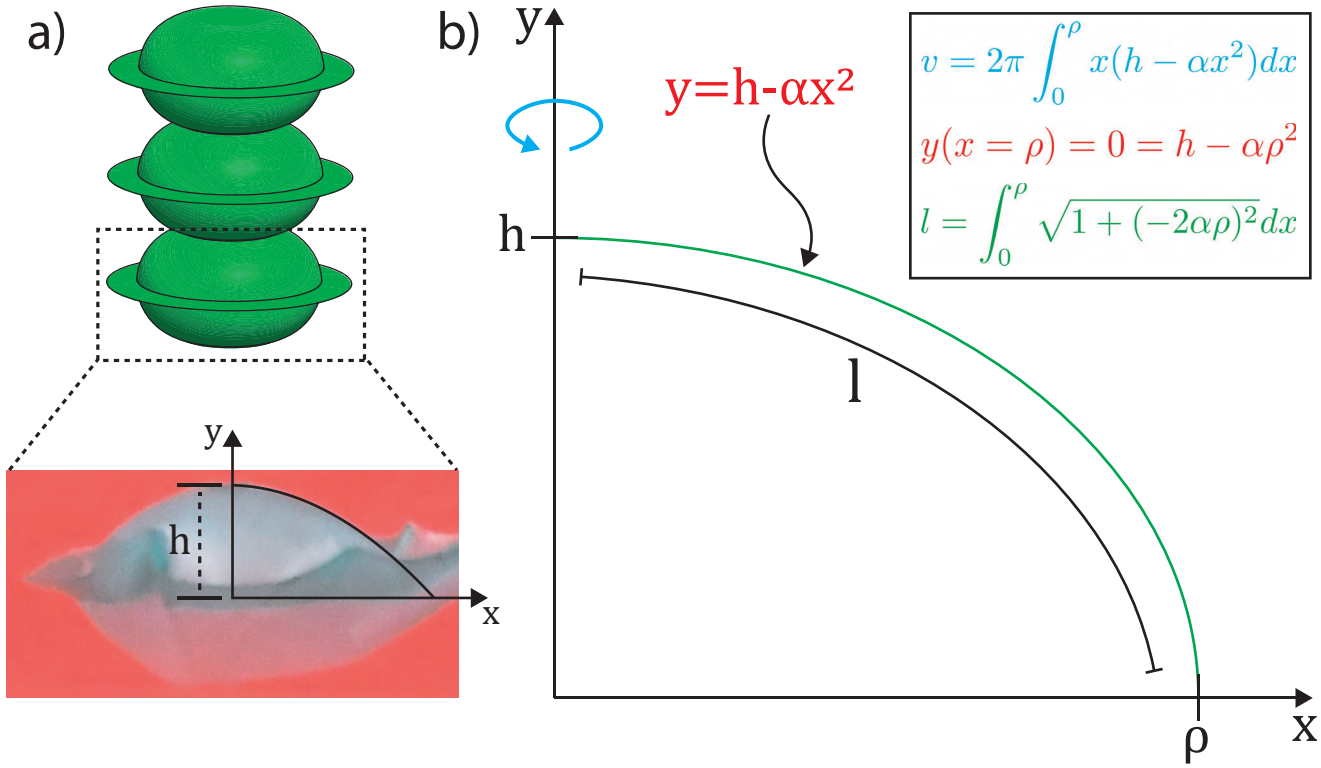

Figure S1: Considerations for geometric modeling of a SBA balloon. a) A single balloon is taken as the base unit of an SBA. We fabricated a single balloon and took a picture of its horizontal cross section. We used MATLAB (MathWorks) image processing tools to fit a variety of curves to the cross section, ultimately determining that parabolas generate the closest fit. b) The first quadrant of a generic parabola is plotted on a set of axes. From this curve, we defined three equations to describe the corresponding SBA balloon. The first equation describes the volume enclosed by the volume of revolution. The second equation is a boundary condition for the parabola equation. The third equation puts a constraint on the balloon's cross sectional arc length.

Using this system of three equations and three variables – v, α, and ρ – we could solve for an approximate relationship between the input volume v and the resulting height h.

The Mathematica notebook reported below shows the steps we took to solve the system.
In section (a) of the code, we defined a function for a Taylor series expansion of the ArcSinh function, which would be used later in the notebook.
We defined the system of three equations in section (b) of the code, and then we solved the system in (c-e).
In (f), we separated the variables, removed higher order terms, and retroactively multiplied by a factor of 4 to correct for the removal of higher order terms.

Geometric Modeling of an SBA

Supplement to "*A Collapsible Soft Actuator Facilitates Performance in Constrained Environments*"

Jacob Rogatinsky

a) The following function is a Taylor expansion for the ArcSinh function, which will be used later in the script.

```
In[]:= trigSeries[n_, θ_] := Normal[Series[ArcSinh[θ], {θ, 0, 2 n - 1}]]
```

b) The following system of three equations describe the shape of an individual balloon from an SBA, determined to be parabolic through image processing. Eq1 describes the volume of revolution generated by revolving the parabola about the y-axis. Eq2 sets the arc length of the parabola in the first quadrant to the deflated radius of the balloon. Eqα is the boundary condition of the equation for a parabola when x=ρ.

```
In[]:= eq1 = v == 2 π Integrate[x (h - α x^2), {x, 0, ρ}];
       eq2 = l == Integrate[Sqrt[1 + (2 α x)^2], {x, 0, ρ}][[1]];
       eqα = h/ρ^2;
```

c) The following equation constitutes an intermediate solution. Eqα is substituted into Eq1 for α, and the resulting Eqρ is solved for ρ.

```
In[]:= eqρ = Solve[eq1 /. α → eqα, ρ][[2]][[1]][[2]];
```

d) The following equation solves the resulting system of equations by substituting Eqα and Eqρ into Eq1 for α and ρ, respectively. The resulting EqSol gives a relationship between the height of the balloon, h, and the volume of the balloon, v.

```
In[]:= eqSol = eq2 /. α → eqα /. ρ → eqρ // Simplify
```

$$\text{Out[]=}\quad 2\,h^{3/2}\,l\,\pi == h\sqrt{2\pi}\,\sqrt{1+\frac{2h^3\pi}{v}}\,\sqrt{v}+\frac{v\,\text{ArcSinh}\left[\frac{h^{3/2}\sqrt{2\pi}}{\sqrt{v}}\right]}{\sqrt{h}}$$

e) The following equation substitutes a second order Taylor series, as defined in (a), into EqSol for the ArcSinh term.

```
In[]:= eqSol2 = eqSol /. ArcSinh[h^(3/2) Sqrt[2 π] / Sqrt[v]] → trigSeries[2, x] /. x → h^(3/2) Sqrt[2 π] / Sqrt[v] // Simplify
```

$$\text{Out[]=}\quad 2\,h^{3/2}\,l\,\pi == \frac{h\sqrt{2\pi}\left(-h^3\pi + 3\left(1+\sqrt{1+\frac{2h^3\pi}{v}}\right)v\right)}{3\sqrt{v}}$$

f) The following equation rearranges EqSol2 such that v and h are on separate sides of the equation.

```
In[]:= eqSol3 = Solve[eqSol2, v][[1]][[1]][[2]] // Simplify
```

$$\text{Out[]=}\quad \frac{1}{108\,l^2}\left(32\,h^5 - 24\,h^3\,l^2 + 18\,h\,l^4 + \left(2\,h^2\left(256\,h^8 - 456\,h^6\,l^2 + 378\,h^4\,l^4 - 216\,h^2\,l^6 + 81\,l^8\right)\right)\Big/ \left(4096\,h^{15} - 10\,944\,h^{13}\,l^2 + \frac{27\,891\,h^{11}\,l^4}{2} - 12\,096\,h^9\,l^6 + 7047\,h^7\,l^8 - 2916\,h^5\,l^{10} + 729\,h^3\,l^{12} + \frac{27}{2}\sqrt{-h^{16}\,l^6\left(7\,h^2 - 6\,l^2\right)^2\left(256\,h^4 - 33\,h^2\,l^2 + 108\,l^4\right)}\right)^{1/3} + 2^{2/3}\left(8192\,h^{15} - 21\,888\,h^{13}\,l^2 + 27\,891\,h^{11}\,l^4 - 24\,192\,h^9\,l^6 + 14\,094\,h^7\,l^8 - 5832\,h^5\,l^{10} + 1458\,h^3\,l^{12} + 27\sqrt{-h^{16}\,l^6\left(7\,h^2 - 6\,l^2\right)^2\left(256\,h^4 - 33\,h^2\,l^2 + 108\,l^4\right)}\right)^{1/3}\right)\pi$$

Removing higher order terms and multiplying by a constant factor of 4 to account for their removal, the resulting approximation is $v \simeq \frac{\left(32\,h^5 - 24\,h^3\,l^2 + 18\,h\,l^4\right)\pi}{27\,l^2}$

S2 FEM Model through SOFA

The model from SOFA exploits a mapping between two spaces – the FEM space and the reduced order space – to maximize the tradeoff between simulation speed and accuracy.
In the FEM space, we defined a set of nodes based on a 3D geometry designed in SolidWorks (Dassault Systèmes) and imported to SOFA as a coarse mesh file. In the reduced order space, we defined a curve to describe the robot's imaginary backbone. This curve is defined by nine reference points, each with six degrees of freedom to capture translation and rotation.
We move from the reduced order space to the FEM space at each time step in the simulation to calculate the internal forces at each mesh node based on the overall system forces from inflation pressure. We then map the mesh node forces to the reduced order space to update the position of the reference curve and the mesh visualization. To move from the reduced order space to the FEM space, we use a kinematic relationship between the two spaces.

$$\mathbf{x} = \mathcal{A}(\mathbf{q}) \tag{4}$$

Here, the non-linear function $\mathcal{A}$ maps a given reference point from $\mathbf{q}$ into the corresponding FEM nodes from $\mathbf{x}$. Since our system has nine reference points, $\mathbf{q}$ and $\mathbf{x}$ do in fact become vectors, and the size of the mapping between them is dependent on the number of nodes in the FEM model. We are also interested in the gradient of the function $\mathcal{A}$, since its transpose allows us to move from the FEM space into the reduced order reference space.

$$\mathbf{J}^T\mathbf{f}(\mathbf{x}) = (\frac{\partial \mathcal{A}}{\partial \mathbf{q}})^T\mathbf{f}(\mathbf{x}) \tag{5}$$

From this equation, the transpose Jacobian matrix $\mathbf{J}^T = (\frac{\partial \mathcal{A}}{\partial \mathbf{q}})^T$ allows us to map the internal mesh forces $\mathbf{f}(\mathbf{x})$ found in the FEM space to a set of new reference points in the reduced space. Overall, this system is well-conditioned and can be inverted with a direct solver.
In practice, the system that is solved is based on static equilibrium between elastic forces in the finite element model and pressure forces: $F_{FEM}(\mathbf{x}) + F_{pressure}(\mathbf{x}, \mathbf{p}) = 0$. The elastic forces are non-linear, but introducing a small variation of the node positions allows us to linearize them at each step:

$$F_{FEM}(x + dx) = F_{FEM}(x) + \left(\frac{dF_{FEM}(x)}{dx}\right)dx = F_{FEM}(x) + Kdx \tag{6}$$

Here, K is the tangent matrix of internal forces in the FEM mesh nodes. Additionally, the pressure forces can be decomposed in the following manner:

$$F_{pressure}(x, p) = H(x)^T * p \tag{7}$$

Here, $H(x)^T$ is a rectangular matrix providing the distribution of pressures acting on the mesh nodes. The number of columns equals the number of DoFs of the SBA, and the number of rows equals the number of nodes in the mesh for each chamber. p is the vector of internal pressures in each SBA cavity, and its size equals the number of DoFs of the SBA.
Since the motion of the simulation is defined in the reduced space, the mesh nodes in $\mathbf{x}$ are constrained by the relationship $\mathbf{x} = \mathcal{A}(\mathbf{q})$ and $d\mathbf{x} = Jd\mathbf{q}$. Given this system, any variation in pressure at a given time step causes a variation in the FEM nodes, given by:

$$F_{FEM}(x + dx) + F_{pressure}(x + dx, p + dp) = 0 \tag{8}$$

This new equilibrium equation can be multiplied by the transposed Jacobian of $\mathcal{A}$ to map it to the reduced space:

$$J^T\big(F_{FEM}(x + dx) + F_{pressure}(x + dx, p + dp)\big) = 0 \tag{9}$$

Now we can substitute in the linearization of the FEM forces, as well as the decomposition of the pressure forces and the relationship between $d\mathbf{x}$ and $d\mathbf{q}$:

$$J^T\big(F_{FEM}(x) + KJdq + H(x)^T * (p + dp)\big) = 0 \tag{10}$$

Here we assume that $H(x + dx)^T \approx H(x)^T$. We can reorient this into a linear system to solve:

$$(J^T K J)dq = J^T\big(F_{FEM}(x) + H(x)^T * (p + dp)\big) \tag{11}$$

Here $J^T\big(F_{FEM}(x) + H(x)^T * (p + dp)\big)$ is a known vector, since we know $\mathbf{x}$, $\mathbf{q}$, and $\mathbf{p}$ from the previous step, and we also know the change in pressure $d\mathbf{p}$ between the previous and current step. Additionally, the matrix $J^T K J$ is symmetric definite positive. This allows us to solve for $d\mathbf{q}$ and generate the configuration of the new reduced space reference curve $\mathbf{q} + d\mathbf{q}$. In the following step, the new position vector of the FEM nodes will be computed as $\mathbf{x}_{new} = \mathcal{A}(\mathbf{q} + d\mathbf{q})$.

S3 Gravitational Contribution

We determined that the effect of gravity on actuator force output was negligible. To calculate the effect of gravity, we summed the weight of the deflated actuator with the weight of its working fluid at full inflation.

$$F_{gravity} = g\big(\rho_{fluid} V_{fluid} + m_{SBA}\big) \tag{12}$$

In equation 12, $g = 9.81 \frac{m}{s^2}$, $\rho_{air} = 1.225\ \frac{kg}{m^3}$, $\rho_{water} = 997\ \frac{kg}{m^3}$, $V_{fluid} = 1.85\ mL$, and $m_{SBA} = 0.4\ g$. This calculation yields $F_{gravity} = 0.004\ N$ for air, and $F_{gravity} = 0.022\ N$ for water. In our force characterizations, the measurement errors over all trials ranged from $\pm 0.01\ N$ to $\pm 0.12\ N$, so the force due to gravity falls in the lower end of this range. We therefore deemed gravity's contribution negligible.

S4 Effect of External Forces in ABAQUS

To demonstrate the effect of external forces on a SBA, we generated an Abaqus simulation where a single column SBA is inflated to a pressure of 6 kPa and a force of 12 mN is applied to the tip (see Fig. S2). This simulation is a representation of the stiffness testing reported in Section 4.4 in the paper. As a result, we obtained an effective Young's modulus of $E = 34.0\ kPa$, compared with $E = 35.3\ kPa$ for the experimental stiffness test. Thus, we show that ABAQUS is able to capture the effects of external loading with a 3.7 % error.

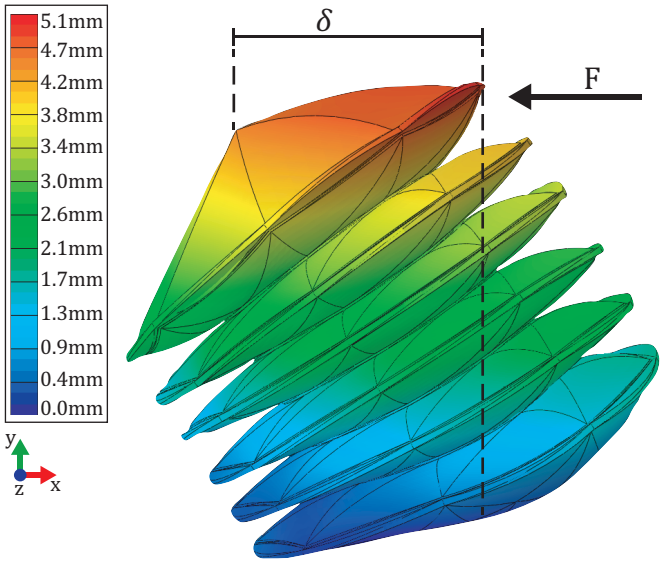

Figure S2: An ABAQUS simulation was developed to mimic stiffness testing on a 1-DoF SBA. Here, we generated an ABAQUS simulation of a 1-DoF SBA of diameter $d = 5\ mm$ and with six balloons.

S5 Experimental Tests Setups

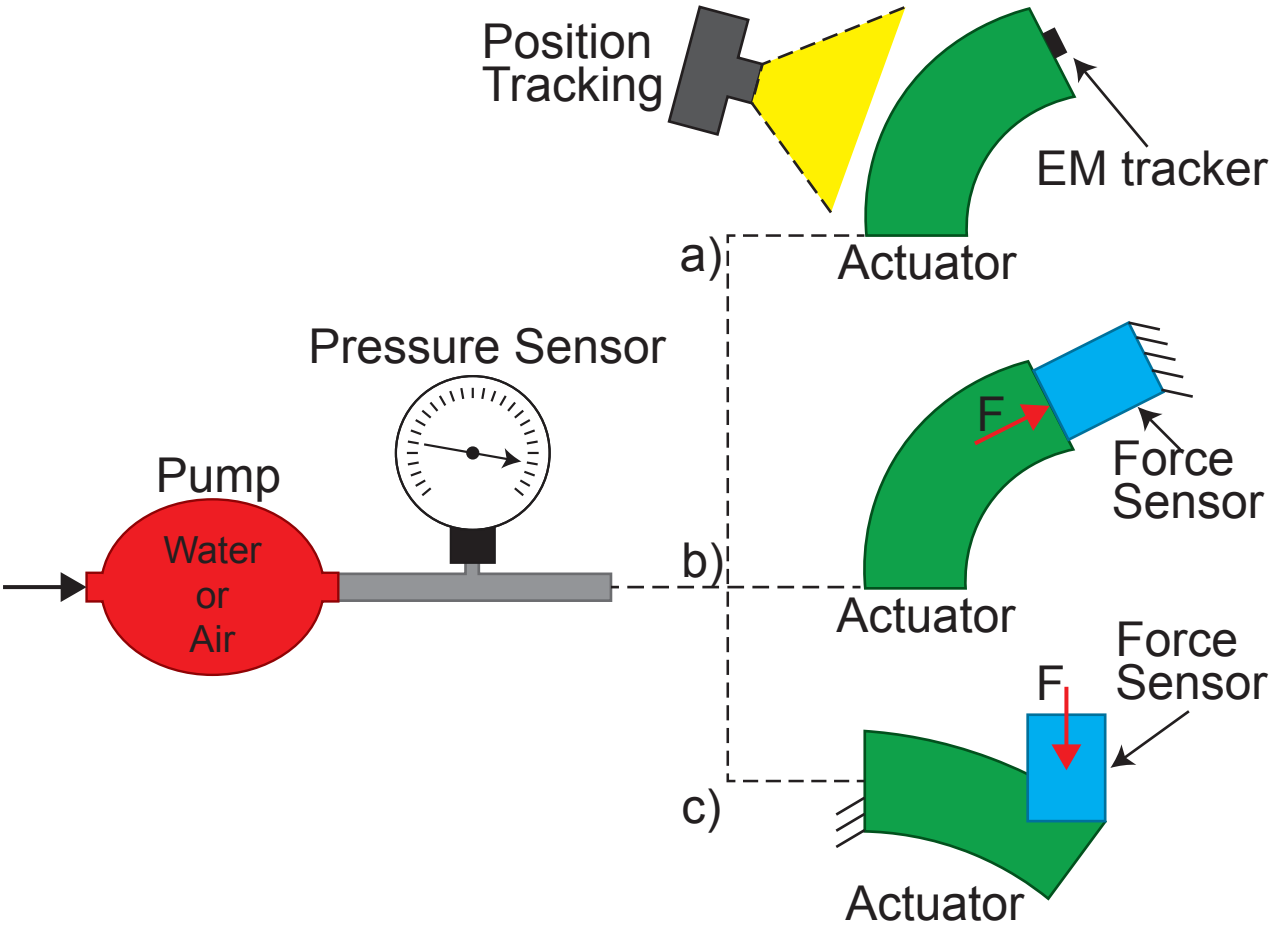

Figure S3: Experimental setups to measure actuator stroke and force output. A pump infuses water or air into the fluidic system at low infusion rates for quasi-static conditions. A syringe pump (Harvard Apparatus, Pump 11 Pico Plus Elite) is used for water, and an air pump (Adafruit, 4699) is used for air. A pneumatic pressure sensor (Honeywell, ASDXAVX030PGAA5) or hydraulic pressure sensor (Nidec Copal Electronics Inc., P-7100-103G-M5) is placed in series between the pump and the soft actuator. a) For the stroke tests, the actuator is allowed to expand freely upon pressurization while an electromagnetic (EM) position tracking system (Northern Digital Inc., Aurora) records its tip position. b) For the force characterizations, a force sensor (ATI Industrial Automation Inc., NANO17) is added to the system in a fixed position and records quasi-static force generation while the actuator inflates into it. c) For the stiffness test, the same force sensor pushes on the actuator while it's held in the inflated position to approximate a cantilevered beam.